

Interference of an array of independent Bose-Einstein condensates

Zoran Hadzibabic, Sabine Stock, Baptiste Battelier, Vincent Bretin, and Jean Dalibard

Laboratoire Kastler Brossel, 24 rue Lhomond, 75005 Paris, France*

(Dated: April 1, 2022)

We have observed high-contrast matter wave interference between 30 Bose-Einstein condensates with uncorrelated phases. Interference patterns were observed after independent condensates were released from a one-dimensional optical lattice and allowed to expand and overlap. This initially surprising phenomenon is explained with a simple theoretical model which generalizes the analysis of the interference of two independent condensates.

PACS numbers: 03.75.Lm, 32.80.Pj

Studies of Bose-Einstein condensates (BECs) loaded into the periodic potential of an optical lattice have been continuously growing in the recent years [1]. These systems have a great potential for a range of applications such as modelling of solid state systems [2, 3, 4, 5, 6], preparation of low-dimensional quantum gases [7, 8], tuning of atom properties [9, 10], trapped atom interferometry [11], and quantum information processing [12, 13].

One of the most commonly used probes of these novel systems are the interference patterns obtained when the gas is released from the lattice, so that the wave packets emanating from different lattice sites expand and overlap [3, 14]. In particular, the appearance of high-contrast interference fringes in the resulting density distribution is commonly associated with the presence of phase coherence between different lattice sites.

In this Letter, we study the interference of a regular array of Bose-Einstein condensates with random relative phases. Independent condensates, each containing $\sim 10^4$ atoms, are produced in a one-dimensional (1D) optical lattice, in the regime where the rate of tunnelling between the lattice sites is negligible on the time scale of the experiment. Contrary to what could be naively expected, we show that high-contrast interference fringes are commonly observed in this system. We present a theoretical model which quantitatively reproduces our experimental results, and show that the periodicity of the lattice is sufficient for the emergence of high-contrast interference patterns, even in the absence of phase coherence between the condensates. This conclusion is independent of the number of sites or the dimensionality of the lattice. Our results generalize the analysis of the interference between two independent condensates [15, 16, 17]. In the last part of the paper we briefly discuss the potential of our system for creating strongly number-squeezed states and report on an unexplained heating effect which occurs for a narrow range of lattice depths.

Our experiments start with a quasipure ^{87}Rb condensate with 3×10^5 atoms in the $F = m_F = 2$ hyperfine state. Condensates are produced by radio-frequency evaporation in a cylindrically symmetric magnetic trap. The harmonic trapping frequencies are $\omega_{\perp}/2\pi = 74\text{ Hz}$ radially, and $\omega_z^{(0)}/2\pi = 11\text{ Hz}$ axially, leading to cigar-

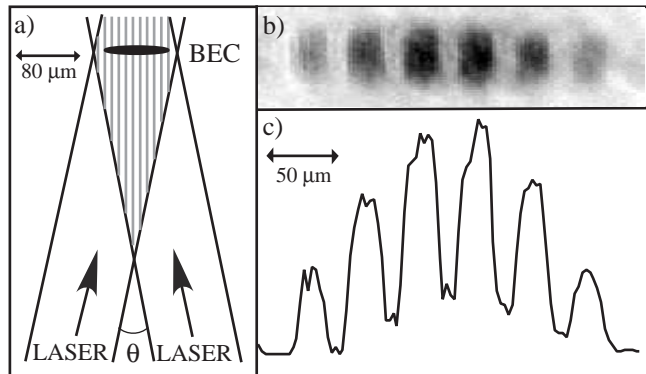


FIG. 1: Interference of Bose-Einstein condensates with uncorrelated phases. (a) A deep 1D optical lattice splits a cigar-shaped condensate into 30 independent BECs. (b) Absorption image of the cloud after 22 ms of expansion from the lattice. The density distribution shows clear interference fringes of high contrast. (c) Axial density profile of the cloud, radially averaged over the central $25\text{ }\mu\text{m}$. The fit described in the text gives a fringe amplitude $A_1 = 0.64$ for this image.

shaped condensates with a Thomas-Fermi length of $L_{\text{TF}} = 84\text{ }\mu\text{m}$, and a radius of $R_{\text{TF}} = 6\text{ }\mu\text{m}$.

We then ramp up the periodic potential created by a 1D optical lattice. The lattice is superimposed on the magnetic trapping potential along the long axis (z) of the cigar (Fig 1a). Two equally polarized laser beams of wavelength $\lambda = 532\text{ nm}$ intersect at an angle $\theta = 0.20\text{ rad}$ to create a standing wave optical dipole potential with a period of $d = \lambda/2 \sin(\theta/2) = 2.7\text{ }\mu\text{m}$. The two beams are focused to waists of about $100\text{ }\mu\text{m}$, and carry a laser power of up to 220 mW each. The blue-detuned laser light creates a repulsive potential for the atoms which accumulate at the nodes of the standing wave, with the radial confinement being provided by the magnetic potential. Along z , the lattice potential has the shape

$$V(z) = \frac{V_0}{2} \cos(2\pi z/d). \quad (1)$$

The lattice depth at full laser power is $V_0/h \approx 50\text{ kHz}$, and the number of occupied sites is $N = L_{\text{TF}}/d \approx 30$.

Thanks to the long lattice period and the large height of the potential barrier between the sites, the 30 condensates can be completely isolated from each other. The

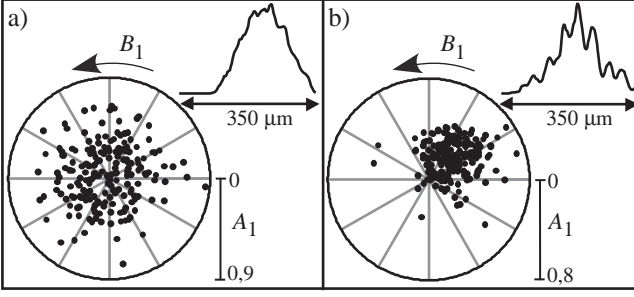


FIG. 2: Polar plots of the fringe amplitudes and phases (A_1, B_1) for 200 images obtained under same experimental conditions. (a) Phase-uncorrelated condensates. (b) Phase-correlated condensates. Insets: Axial density profiles averaged over the 200 images.

matrix element J for the tunnelling between neighboring sites scales as $E_R e^{-2\sqrt{V_0/E_R}}$, where $E_R = \hbar^2 k^2 / 2m = h \times 80$ Hz, $k = \pi/d$, and m is the atom mass. Our maximum lattice depth corresponds to $V_0 \approx 600 E_R$, leading to a timescale \hbar/J of tens of years.

At full lattice depth, the gas at each site is in a quasi 2D regime. The motion along z is “frozen out” because the oscillation frequency $\omega_z/(2\pi)$ is 4 kHz, while the temperature and the chemical potential of the gas correspond to frequencies smaller than 2.5 kHz. Each condensate is therefore in the harmonic oscillator ground state along this direction, with a density distribution given by a Gaussian of width $\ell = \sqrt{\hbar/(2m\omega_z)} = 120$ nm $\ll d$.

In a typical experiment, we ramp up the lattice to $600 E_R$ in $\tau_{\text{ramp}} = 200$ ms. After holding the atoms in the lattice for $\tau_{\text{hold}} = 500$ ms, the optical and magnetic trapping potential are switched off simultaneously, and the density distribution of the cloud is recorded by absorption imaging after $t = 22$ ms of time-of-flight (ToF) expansion. The hold time τ_{hold} is sufficient for the phases of the independently evolving condensates to completely decorrelate (see below). Despite this, the images commonly show clear interference fringes. A spectacular example of this surprising phenomenon is given in Fig. 1b-c, where the contrast is $> 60\%$. Note that high-contrast interference is also observed if the lattice is ramped up before the end of the evaporation sequence, so that the condensates are produced independently at different lattice sites and “have never seen one another” [18].

We analyze the images by fitting the axial density profiles (Fig. 1c) with $[1 + A_1 \cos(B_1 + 2\pi z/D)] G(z)$, where $G(z)$ is a Gaussian envelope. This procedure extracts the first-harmonic modulation of the density distribution, with the fitted fringe period of $39 \mu\text{m}$ in agreement with the expected value $D = \hbar t/(md)$. In Fig. 2a, we summarize our results for 200 consecutively taken images. In most cases the fringe amplitude A_1 is significant, with the mean value $\langle A_1 \rangle = 0.34$, and the standard deviation $\sigma_{A_1} = 0.17$. The fringe phase B_1 is randomly distributed between 0 and 2π . Consequently, no periodic modulation

remains visible if we average the 200 density profiles.

In Fig. 2b, we contrast this with the interference of 30 phase-correlated condensates. Here, we ramp up the lattice in $\tau_{\text{ramp}} = 3$ ms and immediately release the BECs from the trap, before their phases completely diffuse away from each other. In this case, the fringe phases B_1 are clearly not randomly distributed, and the sum of 200 images still shows interference fringes of pronounced contrast. Phase correlations between the separated condensates were lost if the lattice was left on for $\tau_{\text{hold}} \geq 3$ ms.

We have numerically simulated our experiments with phase-uncorrelated condensates using the following model. We consider a 1D array of $N = 30$ BECs initially localized at positions $z_n = nd$ ($n = 1, \dots, N$), and assume that each condensate is in a coherent state described by an amplitude α_n and a phase ϕ_n [19]. We set $\alpha_n \propto n(N-n)$, corresponding to the Thomas-Fermi profile of our BEC at the point when the lattice is switched on. For expansion times $t \gg 1/\omega_z \approx 40 \mu\text{s}$, the atom density at position z is given by [8]:

$$I(z) \propto \left| \sum_{n=1}^N \alpha_n e^{i\phi_n} e^{im(z-z_n)^2/(2\hbar t)} e^{-(z-z_n)^2/Z_0^2} \right|^2 \quad (2)$$

where $Z_0 = \hbar t/(m\ell)$. We neglected the effects of the atomic interactions during the expansion. We perform a Monte-Carlo analysis of $I(z)$ by assigning sets of random numbers to the phases $\{\phi_n\}$. We convolve the resulting density profiles with a Gaussian of $5 \mu\text{m}$ width to account for the finite resolution of our imaging system, and then fit them in the same way as the experimental data. The fitted fringe phase B_1 is randomly distributed between 0 and 2π . For the fringe amplitude we find $\langle A_1 \rangle^{\text{sim}} = 0.31$ and $\sigma_{A_1}^{\text{sim}} = 0.16$, in excellent agreement with the experiment [20].

In order to give a more intuitive explanation of our observations, and generalize our analysis to arbitrarily large N , we now make the following simplifications. We assume that all condensates contain the same average number of atoms, $\alpha_n = \alpha$, and that the expansion time t is large, so that $\ell, z_n \ll Z_0, \sqrt{\hbar t/m}$. In this case, Eq. (2) can be rewritten in the form $I(z) \propto N\alpha^2 e^{-2z^2/Z_0^2} F(z)$, where

$$F(z) = 1 + \sum_{n=1}^{N-1} A_n \cos(B_n + 2\pi n z/D) \quad (3)$$

is a periodic function with period $D = \hbar t/(md)$ and average value 1. $F(z)$ contains all the information about the contrast of the interference pattern. The amplitude A_n and the phase B_n of the n -th harmonic of $F(z)$ are given by the modulus and the argument of $(2/N) \sum_{j=n+1}^N e^{i(\phi_j - \phi_{j-n})}$.

If the N condensates have the same phase, $F(z)$ corresponds to the usual function describing the diffraction

of a coherent wave on a grating

$$F(z) = \frac{1}{N} \frac{\sin^2(N\pi z/D)}{\sin^2(\pi z/D)}. \quad (4)$$

In this case, $F(z)$ has sharp peaks of height N and width $\sim 1/N$ at positions $z = pD$, where p is an integer. In between the peaks, $F(z) \sim 0$.

For the case of uncorrelated phases $\{\phi_n\}$, using Monte-Carlo sampling, we find for $10 \leq N \leq 10^4$:

$$\langle F_{\max} \rangle \sim 1.2 \ln(N) \gg 1 \quad \langle F_{\min} \rangle \sim \frac{0.2}{N} \ll 1 \quad (5)$$

where F_{\max} and F_{\min} are the maximum and the minimum “single-shot” values of $F(z)$, *i.e.* for a given set $\{\phi_n\}$. This shows that even for very large N , most single-shot $F(z)$ are strongly modulated, with a contrast of almost 100%. Since $F(z)$ is also periodic with period D , each single-shot has the qualitative appearance of a high-contrast interference pattern normally expected in the coherent case. However, the exact shape of $F(z)$ and the position of its extrema vary randomly from shot to shot.

The harmonic content of single-shot $F(z)$ is given by $C_n = \langle A_n^2 \rangle = 4(N - n)/N^2$, each A_n resulting from summing $N - n$ complex numbers with random phases and moduli $2/N$. The large modulation of $F(z)$ for $N \rightarrow \infty$ can be understood by noting that while the weight of each harmonic decreases, their number increases [21]. It is interesting to contrast this with averaging N shots of two-condensate interference with an irreproducible phase [22]. In the latter case, the weight of the first harmonic is similar ($\sim 1/\sqrt{N}$), but the absence of higher harmonics leads to a vanishing contrast for large N .

We obtain similar results if we choose for the initial state a Mott insulator with exactly one atom per lattice site (see also [23]). In this case, the signal after ToF consists of the set of coordinates ζ_1, \dots, ζ_N where the N atoms are detected, and its harmonic content is given by:

$$C_n = \frac{4}{N(N-1)} \sum_{j=1}^N \sum_{j' \neq j} \left\langle e^{i2\pi(\zeta_j - \zeta_{j'})n/D} \right\rangle$$

where $\langle \dots \rangle$ now denotes a quantum average. A simple calculation gives $C_n = 4(N - n)/[N(N - 1)]$.

All our arguments naturally extend into two and three dimensions. In 3D, the function generalizing Eq. (3) is $F(\mathbf{r}) = 1 + \sum_{\mathbf{n}} A_{\mathbf{n}} \cos(B_{\mathbf{n}} + 2\pi \mathbf{n} \cdot \mathbf{r}/D)$ where $\mathbf{n} = (n_x, n_y, n_z)$ is a triplet of integers. This is a periodic function in x, y, z with a period D . A Monte-Carlo analysis for a cubic lattice with $20 \times 20 \times 20$ sites with random phases shows that $F(\mathbf{r})$ is again strongly modulated, with $\langle F_{\max} \rangle \simeq 12$ and $\langle F_{\min} \rangle \ll 1$.

In the experimental study of the superfluid to Mott insulator transition with cold atoms [3, 7], the disappearance of interference fringes is observed in the insulating

domain, and used as one of the signatures for the loss of long range phase coherence. This seems in contradiction with our results. However one can reconcile the two findings by noticing that the experiments [3, 7] are performed with a 3D system, observed by integrating the spatial distribution $I(\mathbf{r})$ along the line of observation z . In this case, only the harmonics $(n_x, n_y, 0)$ are observed. In a 3D experiment performed with $N_x \times N_y \times N_z$ sites, the integration along z thus reduces the modulation amplitude by $\sqrt{N_z}$. In fact, the effect is similar to that of averaging N_z images in a 2D experiment, performed with $N_x \times N_y$ sites [24].

In the next part of this Letter, we briefly discuss the potential of our setup for producing “number-squeezed” states with large occupation numbers [14], where the atom number on each site has a sub-Poissonian distribution with an average value $n_0 \gg 1$ and a standard deviation $\sigma < \sqrt{n_0}$. Such states are important for atom interferometry and precision measurements [27].

For simplicity, we restrict our discussion to the case of translational invariance, without the quadratic magnetic potential applied along the z -axis. In the ground state of the system, the squeezing of the atom number on each site depends on the ratio of the tunnelling rate $\tilde{t} = n_0 J/h$ and the effective strength of the repulsive on-site interactions $U \sim \mu/n_0$, where μ is the chemical potential. To give a sense of scale, in our case $n_0 \sim 10^4$ and $U/h \sim 0.2$ Hz. We can qualitatively distinguish three regimes [14, 28]: (i) For $J \geq n_0 U$, squeezing is negligible and the atom number on each site follows a Poissonian distribution ($\sigma = \sqrt{n_0} \sim 100$). (ii) For $J \sim U$ ($\tilde{t} \sim 200$ Hz), squeezing is significant and σ is reduced to $n_0^{1/4} \sim 10$. (iii) Finally, a phase transition to a Mott insulator state with $\sigma < 1$ occurs for $J \sim U/n_0$ ($\tilde{t} \sim 0.2$ Hz).

In our setup, we can tune the value of J across this full range, and the criterion for the Mott transition with $n_0 \sim 10^4$ atoms per site is satisfied for $V_0 \sim 100 - 150 E_R$. However, we point out two practical difficulties which arise for such large values of n_0 . First, for the system to be in its ground state, all decoherence processes, such as particle loss, must have rates lower than \tilde{t} . Second, the assumed translational invariance must be insured to a sufficient level, so that the potential energies at different lattice sites match to better than $n_0 J = h\tilde{t}$. While it seems difficult to fulfill these criteria for the values of \tilde{t} low enough for the Mott transition to occur, the regime of strong squeezing, $\sigma \lesssim n_0^{1/4}$, should be accessible.

In exploring the range of lattice depths $0 - 150 E_R$, we have also observed an unexplained heating effect. In the region $20 < V_0/E_R < 45$ we observe strong heating of the system which peaks for $V_0/E_R \approx 25$ and 35 (Fig. 3). The peak heating rate (measured from the *radial* size of the cloud after ToF) is ~ 200 nK/s as long as the gas is at least partially condensed. However, once the condensate disappears, heating of the thermal cloud becomes

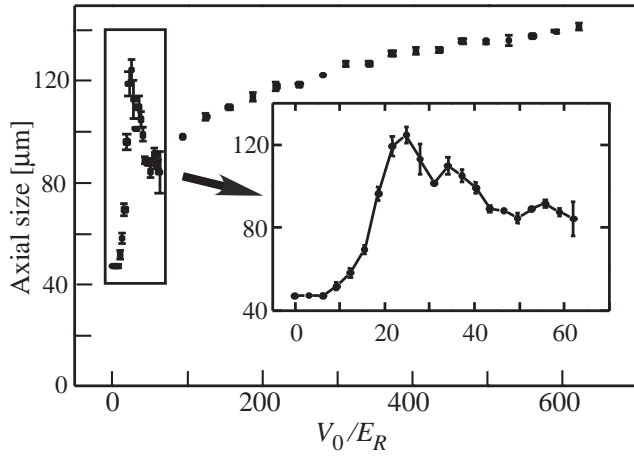


FIG. 3: Axial size of the cloud after 22 ms of expansion as a function of the lattice depth V_0 . Inset: Zoom-in on the region where an unexplained heating of the cloud occurs. For all data points the lattice was raised in $\tau_{\text{ramp}} = 200$ ms and left on for $\tau_{\text{hold}} = 500$ ms before ToF. Error bars are statistical. Outside the heating region, the slow increase of the axial size matches the expected dependence $Z_0 \propto 1/l \propto V_0^{1/4}$.

negligible (< 10 nK/s). Outside $20 < V_0/E_R < 45$, heating due to the lattice is always negligible, independent of the lattice depth or the condensed fraction. We could not attribute this heating to any trivial technical effect. Also, the dynamical instability which occurs at a finite relative velocity between the condensate and the lattice ([29] and refs. therein), should not be relevant here.

In conclusion, we have studied a 1D periodic array of independent condensates prepared in a deep optical lattice. We have shown that most “single-shot” realizations of this system show high-contrast interference patterns in a time-of-flight expansion. We have explained this effect with a simple model which naturally extends to 3D lattices. This initially surprising result should be taken into account in the ongoing studies of atomic superfluidity and coherence in optical lattices, where the contrast of the interference patterns is often used as a diagnostic.

We thank A. Browaeys, T. Esslinger, A. Georges and the ENS group for useful discussions. Z.H. acknowledges support from a Chateaubriand grant, and S.S. from the Studienstiftung des deutschen Volkes, DAAD, and the Research Training Network Cold Quantum Gases HPRN-CT-2000-00125. This work is supported by CNRS, Collège de France, Région Ile de France, and DRED.

[*] Unité de Recherche de l’Ecole normale supérieure et de l’Université Pierre et Marie Curie, associée au CNRS.

[1] I. Bloch, *Physics World*, April 2004, pp. 25-29.

[2] D. Jaksch, C. Bruder, J. I. Cirac, C. W. Gardiner, and P. Zoller, *Phys. Rev. Lett.* **81**, 3108 (1998).

[3] M. Greiner, O. Mandel, T. Esslinger, T. W. Hänsch, and I. Bloch, *Nature* **415**, 29 (2002).

- [4] J. Hecker-Denschlag, J. E. Simsarian, H. Häffner, C. McKenzie, A. Browaeys, D. Cho, K. Helmerson, S. L. Rolston, and W. D. Phillips, *J. Phys. B* **35**, 3095 (2002).
- [5] F. S. Cataliotti, S. Burger, C. Fort, P. Maddaloni, F. Minardi, A. Trombettoni, A. Smerzi, and M. Inguscio, *Science* **293**, 843 (2001).
- [6] O. Morsch, J. H. Müller, M. Cristiani, D. Ciampini, and E. Arimondo, *Phys. Rev. Lett.* **87**, 140402 (2001).
- [7] T. Stöferle, H. Moritz, C. Schori, M. Köhl, and T. Esslinger, *Phys. Rev. Lett.* **92**, 130403 (2004); M. Köhl, H. Moritz, T. Stöferle, C. Schori, and T. Esslinger, *cond-mat/0404338* (2004).
- [8] P. Pedri, L. Pitaevskii, S. Stringari, C. Fort, S. Burger, F. S. Cataliotti, P. Maddaloni, F. Minardi, and M. Inguscio, *Phys. Rev. Lett.* **87**, 220401 (2001).
- [9] B. Eiermann, T. Anker, M. Albiez, M. Taglieber, P. Treutlein, K. P. Marzlin, and M. K. Oberthaler, *cond-mat/0402178* (2004).
- [10] I. Bloch, private communication.
- [11] Y. Shin, M. Saba, T. A. Pasquini, W. Ketterle, D. E. Pritchard, and A. E. Leanhardt, *Phys. Rev. Lett.* **92**, 050405 (2004).
- [12] S. Peil, J. V. Porto, B. L. Tolra, J. M. Obrecht, B. E. King, M. Subbotin, S. L. Rolston, and W. D. Phillips, *Phys. Rev. A* **67**, 051603 (2003).
- [13] H. Ott, E. de Mirandes, F. Ferlaino, G. Roati, V. Türec, G. Modugno, and M. Inguscio, *cond-mat/0404201* (2004).
- [14] C. Orzel, A. K. Tuchman, M. L. Fenselau, M. Yasuda, and M. A. Kasevich, *Science* **291**, 2386 (2001).
- [15] J. Javanainen and S. M. Yoo, *Phys. Rev. Lett.* **76**, 161 (1996).
- [16] M. Naraschewski, H. Wallis, A. Schenzle, J. I. Cirac, and P. Zoller, *Phys. Rev. A* **54**, 2185 (1996).
- [17] Y. Castin and J. Dalibard, *Phys. Rev. A* **55**, 4330 (1997).
- [18] P. W. Anderson, in *The Lesson of Quantum Theory*, edited by J. de Boer, E. Dal, and O. Ulfbeck (Elsevier, Amsterdam, 1986).
- [19] This is equivalent to each condensate being in a Fock state, with the atom number following a Poisson distribution with a mean value α_n^2 (see e.g. [17]).
- [20] The unconvolved, “perfect resolution” profiles give $\langle A_1 \rangle^{\text{sim}} = 0.43$ and $\sigma_{A_1}^{\text{sim}} = 0.22$.
- [21] In practice, this means that a large modulation of $F(z)$ will be observed only if the imaging resolution is sufficient to detect a significant fraction of the harmonics.
- [22] M. R. Andrews, C. G. Townsend, H.-J. Miesner, D. S. Durfee, D. M. Kurn, and W. Ketterle, *Science* **275**, 637 (1997).
- [23] E. Altman, E. Demler, and M. D. Lukin, *cond-mat/0306226* (2003).
- [24] We also stress that the effects discussed here differ from the low-contrast interference which can arise in the Mott regime due to inhomogeneity of the system [25] or incomplete isolation between the lattice sites [26].
- [25] V. A. Kashurnikov, N. V. Prokof’ev, and B. V. Svistunov, *Phys. Rev. A* **66**, 031601(R) (2002).
- [26] R. Roth and K. Burnett, *Phys. Rev. A* **67**, 031602(R) (2003).
- [27] P. Bouyer and M. A. Kasevich, *Phys. Rev. A* **56**, R1083 (1997).
- [28] W. Zwerger, *J. Opt. B* **5**, S9 (2003).
- [29] L. Fallani, L. D. Sarlo, J. E. Lye, M. Modugno, R. Saers, C. Fort, and M. Inguscio, *cond-mat/0404045* (2004).